



ISSN NO. 2320-5407

Journal Homepage: - [www.journalijar.com](http://www.journalijar.com)

## INTERNATIONAL JOURNAL OF ADVANCED RESEARCH (IJAR)

Article DOI: 10.21474/IJAR01/12020  
DOI URL: <http://dx.doi.org/10.21474/IJAR01/12020>



INTERNATIONAL JOURNAL OF  
ADVANCED RESEARCH (IJAR)  
ISSN 2320-5407  
Journal Homepage: <http://www.journalijar.com>  
Journal DOI: 10.21474/IJAR01

### RESEARCH ARTICLE

#### STRUCTURAL, MORPHOLOGICAL AND VIBRATIONAL STUDIES OF MAGNESIUM DOPED LITHIUM TITANATE ANODE MATERIALS FOR LI-ION BATTERIES

D. Vijaya Lakshmi<sup>1</sup>, B. Vikram Babu<sup>2</sup>, M. Sushma Reddi<sup>3</sup>, M. K. Raju<sup>4</sup>, A. Rama Krishna<sup>5</sup>, K. Samatha<sup>6</sup> and P.V. Lakshmi Narayana<sup>1</sup>

1. Department of Nuclear Physics, Andhra University, Visakhapatnam, 530003, India.
2. Department of Physics, Aditya Engineering College (A), Kakinada, 533005, India.
3. Department of Physics, Dr. B. R. Ambedkar University, Srikakulam, 532410, India.
4. Department of HBS, WISTM Engineering College, Visakhapatnam, 531173, India.
5. Department of ECE, Aditya College of Engineering and Technology, Kakinada, 533005, India.
6. Department of Physics, Andhra University, Visakhapatnam, India -530003.

#### Manuscript Info

##### Manuscript History

Received: 05 September 2020  
Final Accepted: 10 October 2020  
Published: November 2020

##### Key words:-

Anode Material, TG/DTG, XRD, SEM, FT-IR

#### Abstract

In the present paper, we study the results of the substitution of Mg<sup>2+</sup> in Li<sub>4</sub>Ti<sub>5</sub>O<sub>12</sub> anode materials with the chemical composition of Li<sub>4-x</sub>Mg<sub>x</sub>Ti<sub>5</sub>O<sub>12</sub> with x = 0, 0.1 and 0.3. Spinel structured Li<sub>4-x</sub>Mg<sub>x</sub>Ti<sub>5</sub>O<sub>12</sub> materials are prepared by conventional ceramic method. The structural, morphological, chemical composition and vibrational studies of the prepared anode samples are systematically characterized by thermal analysis, XRD, SEM, EDS and FT-IR. Phase formation is confirmed by thermal analysis followed by the XRD and FT-IR spectroscopic results. The X-ray diffraction (XRD) technique exposed that the materials belonged to spinel type having the space group as Fd-3m. Synthesized samples are quite large upto 0.98 to 1.3 μm in diameter and the grain size had a wide distribution range. EDS is used to identify the elements. The FT-IR spectra show tetrahedral and octahedral sites to be inhabited by the MO<sub>6</sub> oxide lattice.

*Copy Right, IJAR, 2020,. All rights reserved.*

#### Introduction:-

Constant increase in demand for energy storage systems continued with rapid development of electric vehicles (EVs) and hybrid electric vehicles (HEVs). The rechargeable LIBs have become primary choice due to its high energy density, good rate capability, safety and long cycle life. In the last decade, most attention has been paid to the search for alternative negative electrode materials instead of the commercial graphite [1-3].

The spinel structured Lithium titanate (Li<sub>4</sub>Ti<sub>5</sub>O<sub>12</sub>, LTO) is the most promising anode material due its low toxicity and cost, excellent thermal stability in the fully charged state and high capacity. Nevertheless, Li<sub>4</sub>Ti<sub>5</sub>O<sub>12</sub> suffers from the low electronic conductivity and diffusivity which increases the impedance of the electrode and decreases the rate performance. This significantly limits their applications in LIBs [4-8].

To conquer these conductivity shortcomings of Li<sub>4</sub>Ti<sub>5</sub>O<sub>12</sub>, transition metals and rare earth elements for example Ca<sup>2+</sup>, Cu<sup>2+</sup>, Mg<sup>2+</sup>, Zn<sup>2+</sup>, Al<sup>3+</sup>, Cr<sup>3+</sup>, Co<sup>3+</sup>, Fe<sup>3+</sup>, Ga<sup>3+</sup>, La<sup>3+</sup>, Y<sup>3+</sup>, Mn<sup>4+</sup>, Ru<sup>4+</sup>, Zr<sup>4+</sup>, Nb<sup>5+</sup>, Ta<sup>5+</sup>, V<sup>5+</sup> and Mo<sup>6+</sup> in

Lithium and Titanium sites can be used as substituents. Among all these, Magnesium is very inexpensive and anticipated to even out the structure, it has been chosen as a dopant for Lithium site [9-14]. In the structure, the doping of divalent state of Magnesium for monovalent state of Lithium requires that the charge difference is adjusted by lessening corresponding number of Titanium ions from  $Ti^{4+}$  to  $Ti^{3+}$ . This resulted not only in amplification of  $Li_4Ti_5O_{12}$  conductivity but also in the electrochemical efficiency relative to the  $Li_4Ti_5O_{12}$  material.

The cubic spinel structure of LTO is represented as is  $Li_{8a}[Ti_{5/3}Li_{1/3}]_{16d}O_4$ , in this case 75% of the  $Li^+$  are placed in tetrahedral 8a sites, while the residual ions are like  $Li^+$  and  $Ti^{4+}$  as positioned at the 16c octahedral sites of symmetry group with Fd3m [15-17]. In this chemical reaction process the tetrahedral-position of  $Li^+$  freely moves into neighboring 16c octahedral positions to create a Rock salt structure  $(Li_2)_{16c}(Ti_{5/3}Li_{1/3})_{16d}O_4$ . Mg is chosen for substituting in LTO as Li and Ti lattice sites are not altered in  $Li_{4-x}Mg_xTi_5O_{12}$  prepared through the solid state method [18-21]. Here we reported the synthesis and structural properties of the Mg doped  $Li_4Ti_5O_{12}$  anode materials to understand the phase, morphology and vibrational properties.

#### Preparation and Experimental Characterizations:

The anode material compositions are prepared through solid state route from stoichiometric ratios of  $Li_2CO_3$ ,  $TiO_2$ , and MgO is taken as the raw material from the Himedia with purity of 99.9%.

A three percentage of surplus quantity of  $Li_2CO_3$  is put to use so as to nullify any sort of loss of the material which might have taken place in the process of heating. Initially the unprocessed materials are methodically mixed by making use of agate and mortar; further methanol is added to obtain homogeneity of the materials and grinded for 8h. The material is calcined for 20 hours in air at 850 °C utilizing a programmable furnace to dry the compounds from any impurities. The samples are cooled to ambient temperature and then ground for 2 hours in the mortar again so as to arrive at the final powder.

The TG and DTG measurements are taken by Mettler Toledo TG/DTG 851° instrument from 30-1000 °C in  $N_2$  atmosphere at a heating rate of 10°C /minute. The XRD properties of the samples are studied by Rigaku X-ray diffractometer using the  $CuK\alpha$  radiation (wavelength = 1.54 Å) containing diffraction angle range from 10° to 90° with successive 0.02° angular increments. The morphology of the material grains is observed using FESEM micrographs taken from CarlZeiss, EVOMA 15, Oxford Instruments, Inca Penta FETx3.JPG. FT-IR spectra are extracted by making use of a Shimadzu IR-Prestige21 spectrometer utilizing the methodology of KBr pellet in the wavenumber ranging between 400 and 4000  $cm^{-1}$ .

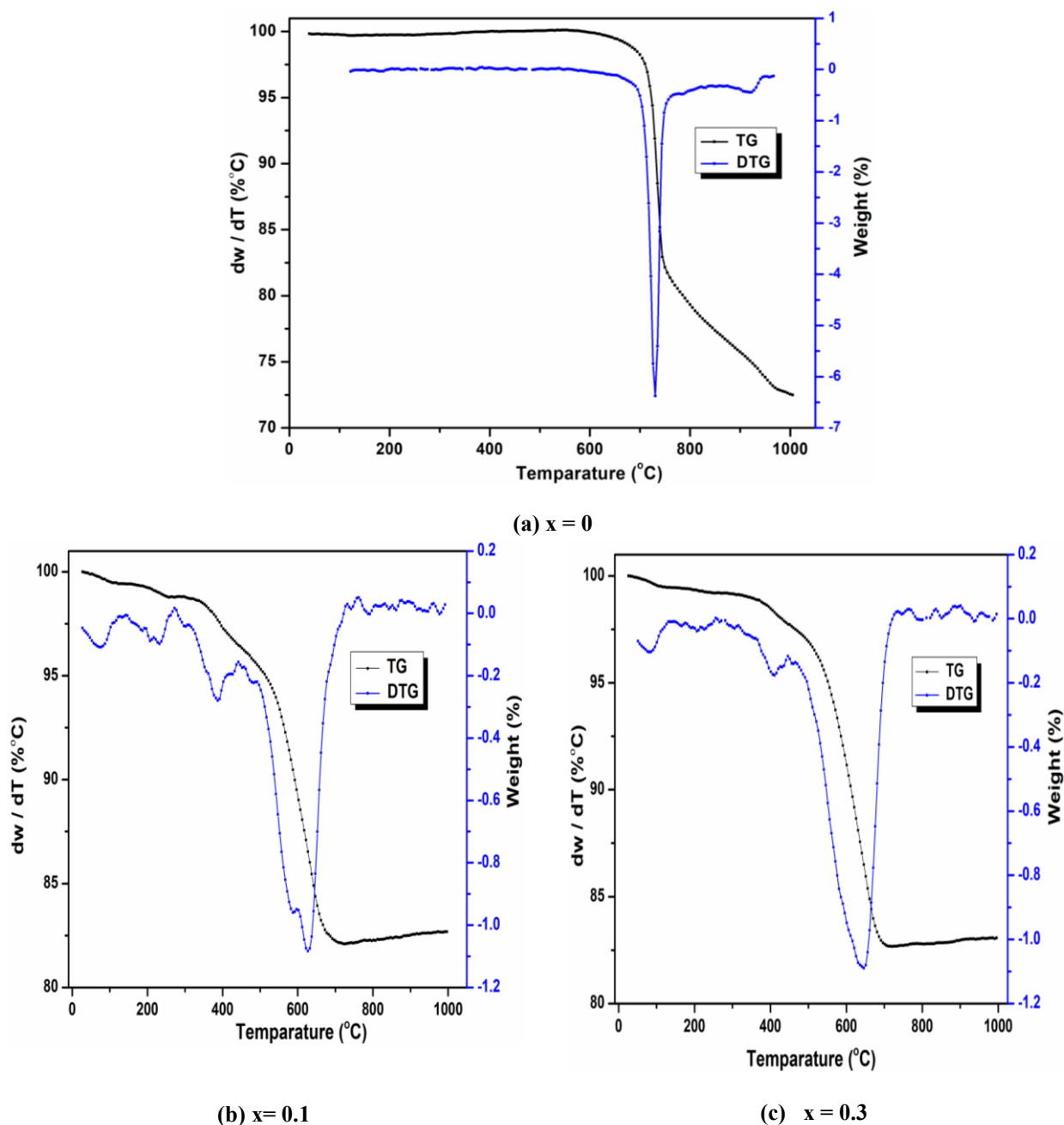
### Results and Discussion:-

#### Thermal Studies:

Figures 1(a)-1(c) show TG and DTG plots for Magnesium substituted in LTO compounds. In response to the difference in the ratio of Magnesium doped, there is little difference in the three graphs. From the TG/DTG curves, it is shown that there is no loss of weight from room temperature to 400 °C. The total mass loss of LTO is approximately above the 20% which is high for the Mg substituted materials in LTO. The Mg substituted Lithium titanate materials of TG profiles show the overall loss of weight is (17%) assessed between 400 °C and 700 °C.

The initial mass loss observed from the TG curves from 300 °C to 500 °C is approximately 2.5 %. This is corresponding to the loss of moisture content absorbed on the surfaces and some intercalated water molecules during grinding and methanol used in the synthesis process with a little difference in the curves. All the TG/DTG curves obtained from Mg substituted precursors indicated that there is a maximum weight loss of the samples, decreases quickly between 600 °C and 700 °C suggesting that the complicated reactions of decomposition of the of inorganic materials such as the precursors of Lithium carbonate, Titanium oxide and Magnesium oxide decomposed materials [18-22].

TG curves of  $Li_{4-x}Mg_xTi_5O_{12}$  series show that the major weight or mass loss (15%) is between 600 °C and 700 °C temperatures. The corresponding peaks are seen at ~ 630°C (for LTO it is observed ~ 730 °C) on the DTG curves. From all the TG curves, a negligible weight loss is seen above 700 °C to 1000 °C, which indicates that the spinel crystalline structures of  $Li_{4-x}Mg_xTi_5O_{12}$  have formed around 850 °C approving with the selected temperature condition [17, 23-25].



Figures 1(a) - 1(c):-TG/ DTG graphs for  $\text{Li}_{4-x}\text{Mg}_x\text{Ti}_5\text{O}_{12}$  ( $x = 0, 0.1$  and  $0.3$ ) compounds.

#### XRD Analysis:

The XRD graphs of  $\text{Li}_{4-x}\text{Mg}_x\text{Ti}_5\text{O}_{12}$  ( $x = 0, 0.1, \text{ and } 0.3$ ) anode materials, calcined at  $850^\circ\text{C}$  for 20 hours in air, are shown in figure 2. Every peak of diffraction is quite narrow and sharp, depicting the materials to be of the crystalline type. From the XRD graphs, the diffraction spectra of the un-doped and doped materials of the diffraction peaks are good and consistent with PDF card # 49-0207, which had similar characteristics of cubic LTO crystal system [14, 24-27]. From the X-ray Diffraction figures, it can be observed that all the peaks of Magnesium substituted materials are comparable to those of pristine LTO.

From the XRD graph all the diffraction peaks of the  $hkl$  values are (111), (2 2 0), (3 1 1), (2 2 2), (4 0 0), (3 3 1), (3 3 3), (4 4 0), (5 3 1), (5 3 3), (6 2 2), (4 4 4) (5 5 1) and (7 3 1) indexed as clearly identifiable with base material LTO.

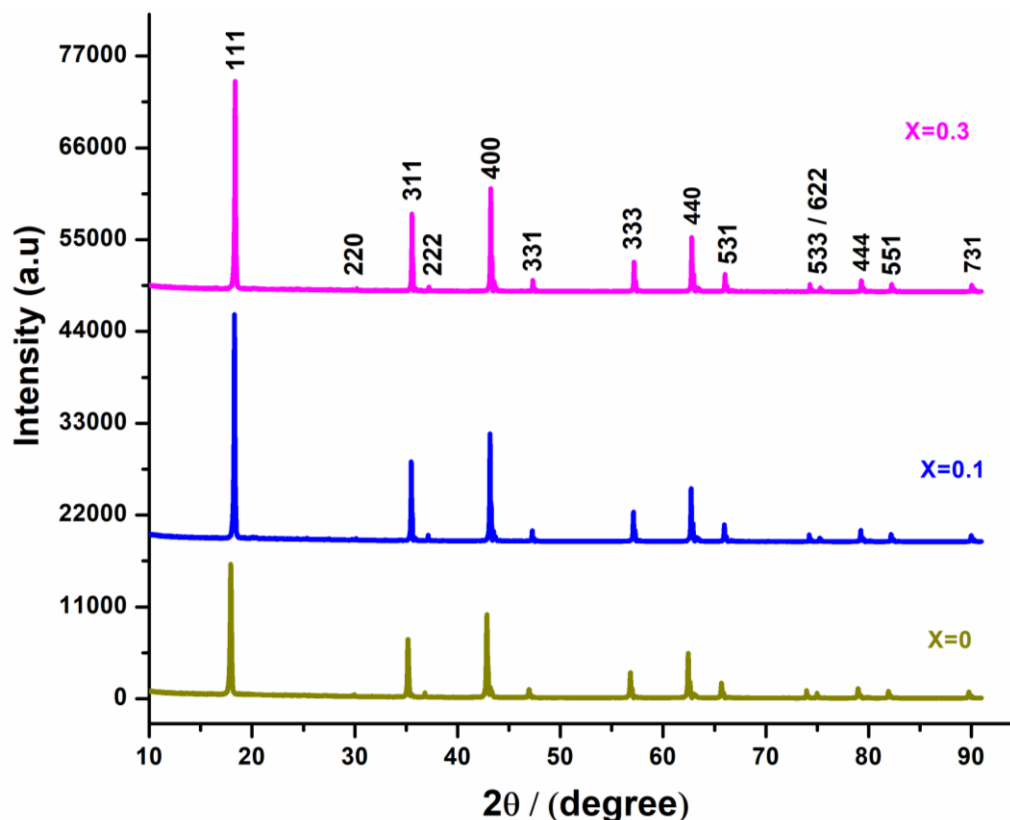


**Figure 2:-** XRD patterns for  $\text{Li}_{4-x}\text{Mg}_x\text{Ti}_5\text{O}_{12}$  ( $x = 0, 0.1$  and  $0.3$ ) materials.

There is no other impurity peak seen from XRD graph, which indicated that  $\text{Mg}^{2+}$  has effectively entered into the Li site. Absence of impurity peak also confirmed the single phase crystalline nature. After  $\text{Mg}^{2+}$  substitution, the main peak belonging to the (111) index progressively moves from  $18.30^\circ$  to  $18.32^\circ$ . The lattice constant is increased with the dopant composition of Mg [19-21, 28]. The increase of the lattice volume might provide large space for  $\text{Li}^+$  charging and discharging and also can efficiently improve LTO electrical conductivity. Crystallite sizes of the  $\text{Li}_{4-x}\text{Mg}_x\text{Ti}_5\text{O}_{12}$  are estimated by making use of the Debye-Scherrer formula

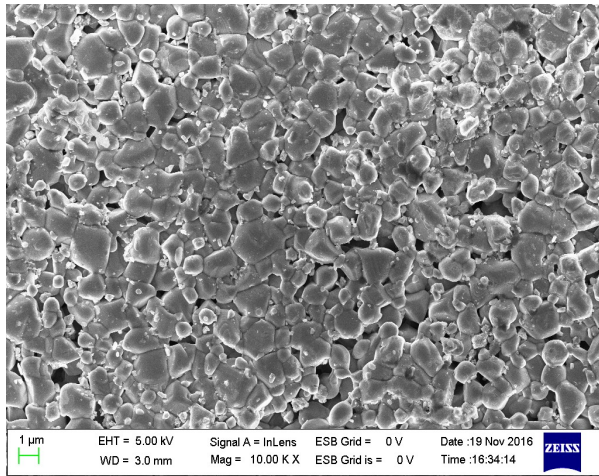
$$L = \frac{k\lambda}{\beta \cos \theta}$$

The lattice constants, crystallite sizes and unit cell volumes are estimated by making use of the UnitCell software (1997) and listed in table 1.

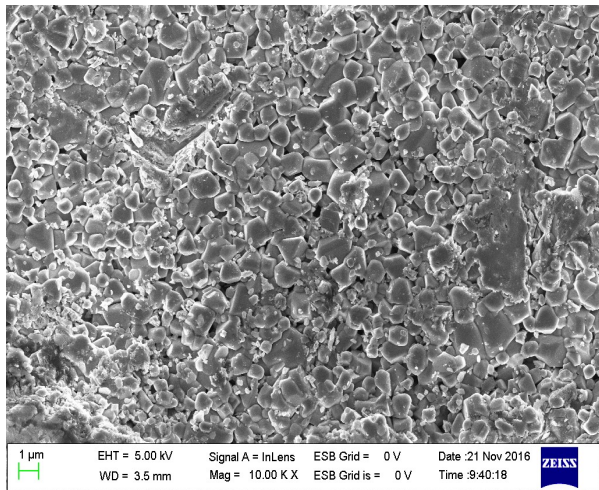
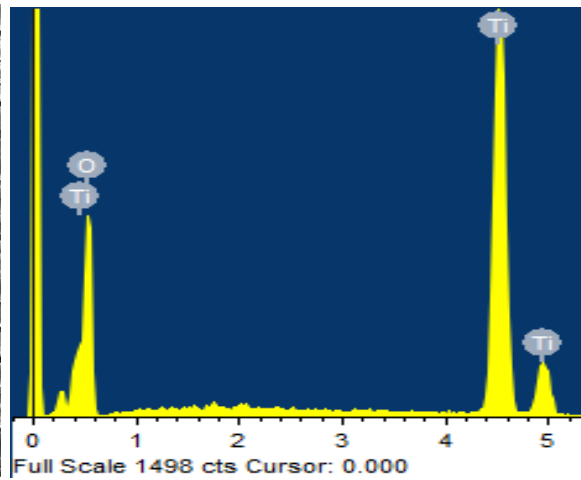
**Table 1:-** Lattice parameters, Unitcell volume and Crystallite sizes and Grain sizes of the prepared  $\text{Li}_{4-x}\text{Mg}_x\text{Ti}_5\text{O}_{12}$  ( $x = 0, 0.1$  and  $0.3$ ) materials.

Materials	Lattice Constant a (Å)	Cell Volume (Å) <sup>3</sup>	$I_{(111)}/I_{(400)}$	Crystallite Size (nm)	Grain Size (μm)
X=0 (LTO)	8.3586	583.9835	1.50	48.08	0.98
X=0.1	8.3645	585.2210	1.65	52.65	1.18
X=0.3	8.3678	585.9138	1.38	56.34	1.3

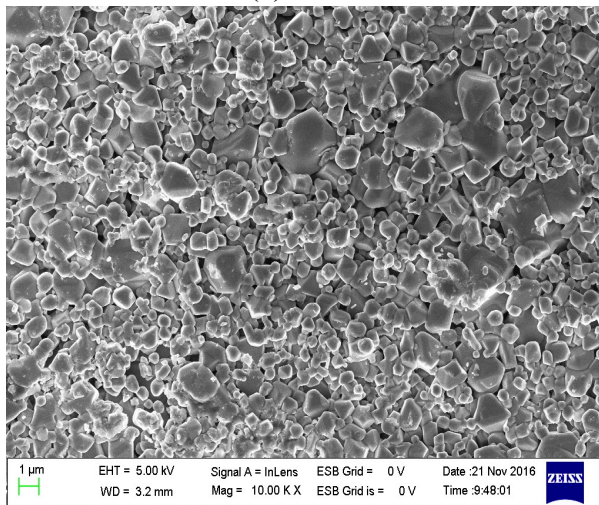
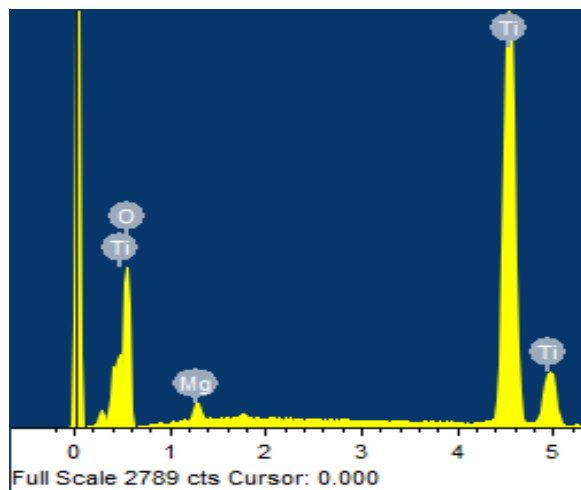
SEM With EDS Analysis:



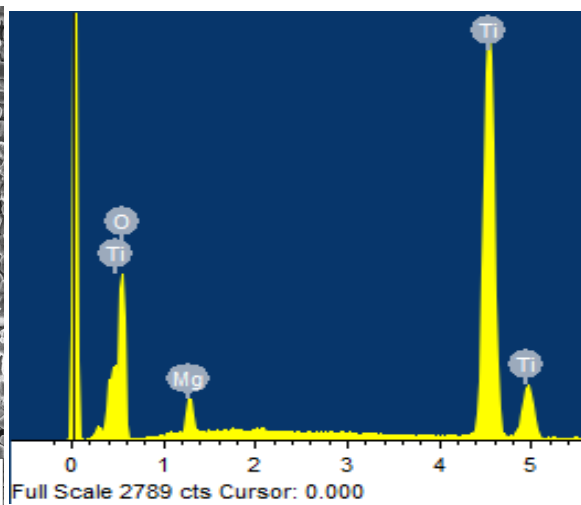
(a)  $x=0$



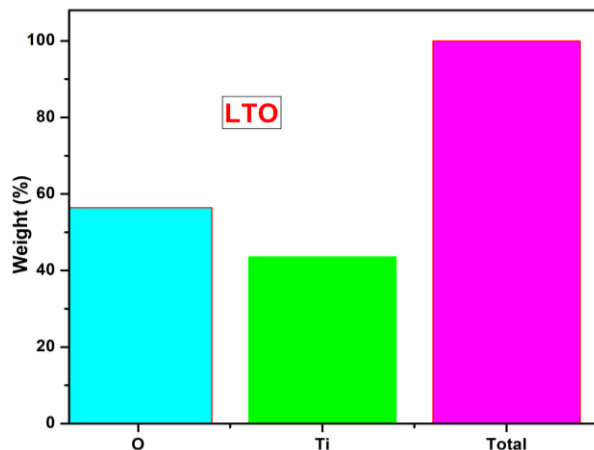
(b)  $x=0.1$



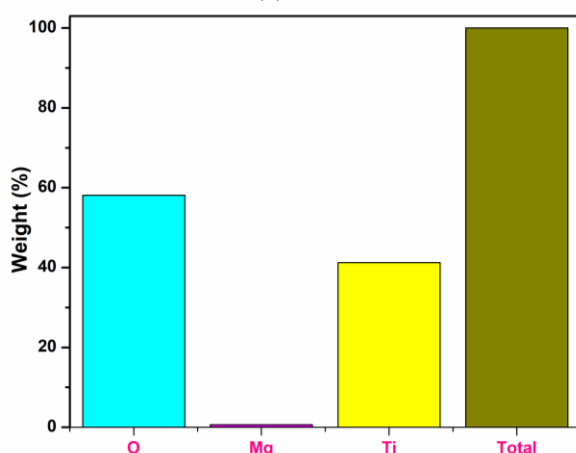
(c)  $x=0.3$



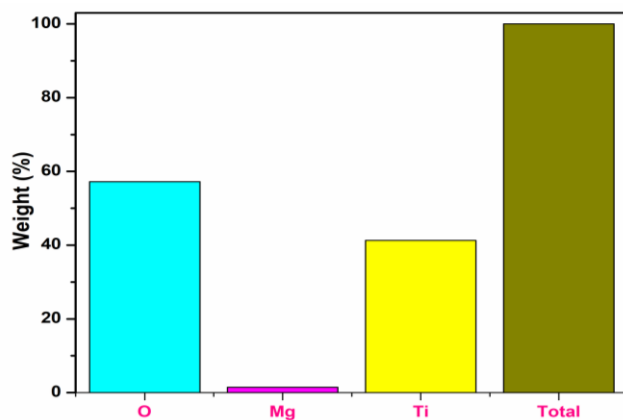
Figures 3(a) - 3(c):- SEM micrographs and EDS images for  $Li_{4-x}Mg_xTi_5O_{12}$  ( $x = 0, 0.1$  and  $0.3$ ) compounds.

(a)  $x=0$ 

Composition	$x=0$	
Element	Weight %	Atomic %
O	56.42	80.21
Ti	43.58	19.79
Total	100	100

(b)  $x=0.1$ 

Composition	$x=0.1$	
Element	Weight %	Atomic %
O	58.12	80.44
Mg	0.60	0.58
Ti	41.28	18.98
Total	100	100

(c)  $x=0.3$ 

Composition	$x=0.3$	
Element	Weight %	Atomic %
O	57.22	80.01
Mg	1.49	1.35
Ti	41.29	18.64
Total	100	100

Figures 4(a) - 4(c):-EDS histogram spectra and composition of elements of  $\text{Li}_{4-x}\text{Mg}_x\text{Ti}_5\text{O}_{12}$  ( $x = 0, 0.1$  and  $0.3$ ) compounds.

The SEM and EDS images of  $\text{Li}_{4-x}\text{Mg}_x\text{Ti}_5\text{O}_{12}$  materials are sintered at  $850^\circ\text{C}$  for 20 hours and these are shown in the figures 3 (a) to 3(c). They show the agglomeration of well-sized crystalline submicron particles with sizes of  $0.98\ \mu\text{m} - 1.3\ \mu\text{m}$  of all samples as shown in table 3.1.

Synthesized material particles are present as larger grains of agglomeration and as the value of  $x$  increase the size of the grains and agglomeration are increased than the base LTO compound. The size difference in the grains increases the amount of surface area inside the anode material, which is potentially causing a much greater charge transference and initial capacity.

As it is well-known, the kinetic property of Li-ion transportation in the particles is limited by ion diffusion pathway. An electrode material has advantage with this unique morphology for the reason that it aids to elevate the electrochemical efficiency [22-25]. From figures 3 (a) to 3 (c) it is clearly visible that particles are spherically in shape. Aggregated view of all these small particles is seen on the surface of the powder. With increase of Mg content, the particle size also increased and there is a distortion in the spherical shape. The small grain sizes are beneficial to improve the electrochemical performance as a result of the shortening of  $\text{Li}^+$  and electron diffusion lengths within the materials [28, 29]. The electrochemical performances of composite electrode with increase of Mg content are found to be better and the experiments conducted are also in support with the theory of high Mg content. These results are in good correlation with XRD studies and the crystallinity is well developed. All the compounds exhibit uniform grain distribution and a small porous structure.

The EDS is a generally utilized technique implemented for investigative examination of essential parametric composition of a sample. In this method, the spectroscopic data are plotted as a graph of counts versus energy. The EDS and quantitative results of  $\text{Li}_{4-x}\text{Mg}_x\text{Ti}_5\text{O}_{12}$  (where  $x = 0, 0.1$  and  $0.3$ ) series compounds are shown in figures 3(a)-3(c) and 4(a)-4(c). As shown in figures 3(a-c) and 4(a-c), there are no other peaks or elements that appeared in the spectra besides Ti, Mg and O in  $\text{Li}_{4-x}\text{Mg}_x\text{Ti}_5\text{O}_{12}$ . The region scanned with EDS is reported in figures 3(a-c), which clearly shows the characteristic peaks or histogram graphs of Ti, Mg and O samples and no other impurity peaks. It is obvious from the EDS results that the characteristic X-ray peaks are due to Ti, Mg and O alone.

#### FTIR Spectroscopic Analysis:

The FTIR patterns of the Magnesium substituted LTO materials scanned in the frequency region from 400 to 4000  $\text{cm}^{-1}$  are shown in the figure 5. From the FTIR figure, it is clearly observed that the irregular layers of trigonally distorted  $\text{MO}_6$  ( $M = \text{Li}, \text{Mg}$  and  $\text{Ti}$ ) are tetrahedra and octahedra bands existing in the  $\text{Li}_{4-x}\text{Mg}_x\text{Ti}_5\text{O}_{12}$  materials compounds. The Wyckoff positions  $8a$  and  $16c$  consist of Li-ions and transition metal (Li, Mg and Ti) ions respectively [14, 15].

**Table 2:-** FTIR band assignments in  $\text{Li}_{4-x}\text{Mg}_x\text{Ti}_5\text{O}_{12}$  ( $x = 0, 0.1$  and  $0.3$ ) compounds.

Composition	Infrared wavenumber ( $\text{cm}^{-1}$ )			
$x=0$	462	572	855	1080
$x=0.1$	463.4	576.7	857.5	1078.6
$x=0.3$	462.8	577.6	859.7	1072
Assignment	(Li-O)	(Ti-O)	(Mg-O)	(Ti-O)

On Magnesium substitution in Lithium titanate the peaks seem to shift towards the higher wavenumber side with the width of the peak increasing as the Mg composition increases. The Mg substituted  $\text{Li}_{4-x}\text{Mg}_x\text{Ti}_5\text{O}_{12}$  series compounds are partitioned into  $\text{LiO}_6$  and  $\text{MO}_6$  layers which are found in the frequency range 400-900  $\text{cm}^{-1}$  [25, 26]. Due to limitations associated with the instrument employed, the IR spectrum for Mg doped LTO is not recorded below the wavenumber of 400  $\text{cm}^{-1}$  to observe the vibrations of  $\text{LiO}_6$ . With the increase of Mg substitution, the stretching and bending mode vibrations also slightly change to higher frequency sides, due to a variation in M-O covalence bond. The Wyckoff positions  $8a$  and  $16c$  consist of  $\text{Li}^+$  ions and transition metal (Li, Mg and Ti) ions respectively [14, 30]. Table 2 shows the vibrational modes and band assignments in Mg doped LTO materials.

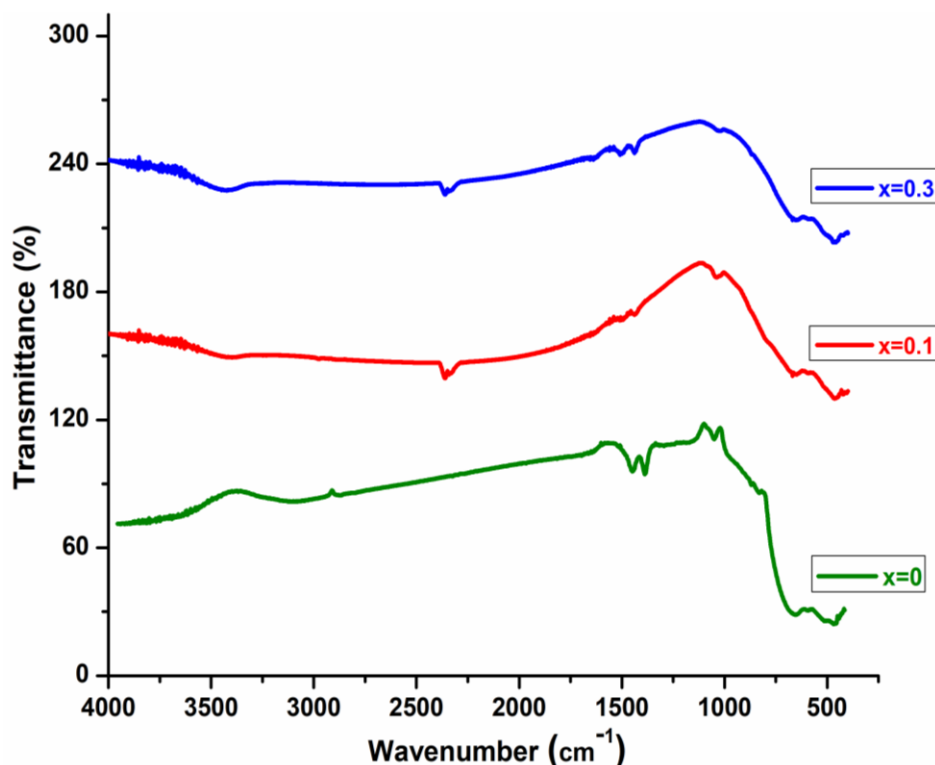


Figure 5:- FTIR spectra for  $\text{Li}_{4-x}\text{Mg}_x\text{Ti}_5\text{O}_{12}$  ( $x = 0, 0.1, \text{ and } 0.3$ ) materials.

### Conclusions:-

In this paper we investigated the structural effects of Vanadium (V) substitution in Titanium (Ti) site of spinel LTO anode materials for LIBs. Various characterizations of the compounds are analyzed by using different experimental characterizations. The structure, composition, morphology and bonding nature of the fabricated materials are characterized by TG/DTG, XRD, SEM with EDS and FT-IR. TG/DTG studies reveal the temperature dependence of the material properties. The Vanadium substituted in spinel  $\text{Li}_{4-x}\text{Mg}_x\text{Ti}_5\text{O}_{12}$  for ( $x = 0, 0.1$  and  $0.3$ ) anode compounds are efficiently prepared via ceramic route at  $850^\circ\text{C}$  for 20 hours. From XRD studies the compounds possess a typical structure of the spinel type having a space group of the Fd-3m class. Fractional substitution of Mg in place of Li enhances the lattice parameter. SEM with EDS is employed to study the microstructures and elemental compositions respectively. All the samples show that porosity nature is observed in SEM analysis. From the SEM images, we observe that the structural, morphological features and grain size distributions are in the range from  $0.98$  to  $1.3\ \mu\text{m}$ . The spectra extracted by making use of FTIR reveal that the structural lattice of oxide includes  $\text{MO}_6$  tetrahedra and octahedra.

### References:-

1. T. Placke, R. Kloepsch, S. Duhnen, M. Winter, "Lithium ion, Lithium metal, and alternative rechargeable battery technologies: the odyssey for high energy density", *J. Solid State Electrochem.*, 21 (2017), pp.1939.
2. M. M. Thackeray, "Structural Considerations of Layered and Spinel Lithiated Oxides for Lithium Ion Batteries", *J. Electrochem Soc.*, 142(8) (1995), pp. 2558.
3. T. Haisheng, Z. Feng, H. Liu, X. Kan, P. Chen, "Reality and Future of Rechargeable Lithium Batteries", *Open Mater Sci. J.*, 5 (2011) pp. 204.
4. C. P. Sandhya, B. John and C. Gouri, "Lithium titanate as anode material for Lithium-ion cells: a review", *Ionics*, 20 (2014) pp. 601.
5. T. Ohzuku, A. Ueda, and N. Yamamoto, "Zero-strain insertion material of  $\text{Li}(\text{Li}/3\text{Ti}5/3)\text{O}_4$  for rechargeable Lithium cells", *J. Electrochem. Soc.*, 142 (1995) pp.1431.
6. G.Q. Liu, L. Wen, G. Y. Liu, Q.Y. Wu, H.Z. Luo, B.Y. Ma, and T.Y. Wen, "Synthesis and electrochemical properties of  $\text{Li}_4\text{Ti}_5\text{O}_{12}$ ", *Journal of Alloys and Compounds*, 509 (22) (2011) pp. 6427.
7. T.Z. Yuan, and W. Peng, "Research progress in electrode material  $\text{Li}_4\text{Ti}_5\text{O}_{12}$ ", *Battery Bimonthly*, 37 (2007) pp. 73.

8. T.F. Yi, L.J. Jiang, J. Shu, C.B. Yue, R.S. Zhu, and H.B. Qiao, "Recent Development and Application of  $\text{Li}_4\text{Ti}_5\text{O}_{12}$  as Anode Material of Lithium Ion Battery", *J. Phys. Chem. Solids*, 71 (2010) pp.1236.
9. Q. Y. Zhang, and X. Li, "Recent Developments in the Doped-  $\text{Li}_4\text{Ti}_5\text{O}_{12}$  Anode Materials of Lithium-Ion Batteries for Improving the Rate Capability", *Int. J. Electrochem. Sci.*, 8 (2013) pp. 6449.
10. S. Y. Feng, W. Feng, and C. C. feng, "Preparation of  $\text{Li}_4\text{Ti}_5\text{O}_{12}$  from Nanocrystalline  $\text{TiO}_2$  and It's Lithiation Performance", *Acta Physico-chimica Sinica*, 20 (2004) pp. 707.
11. V. D. Nithya, S. Sharmila, K. VEDIAPPAN C. W. Lee, L. Vasylechko, and R. K. Selva, "Electrical and electrochemical properties of molten-salt synthesized 0.05 mol Zr-and Si-doped  $\text{Li}_4\text{Ti}_5\text{O}_{12}$  microcrystals", *J. Appl Electrochem*, 44 (2014) pp. 647.
12. K.C. Hsiao, S.C. Liao, J.M. Chen, "Microstructure effect on the electrochemical property of  $\text{Li}_4\text{Ti}_5\text{O}_{12}$  as an anode material for Lithium-ion batteries", *Electrochim. Acta*, 53 (2008) pp.7242.
13. Q. Y. Zhang, and X. Li, "Recent Developments in the Doped-  $\text{Li}_4\text{Ti}_5\text{O}_{12}$  Anode Materials of Lithium-Ion Batteries for Improving the Rate Capability", *Int. J. Electrochem. Sci.*, 8 (2013) pp. 6449.
14. M. Senna, M. Fabian, L. Kavan, M. Zukulova, J. Briancin, E. Turianicova, P. Bottke, W.V. Sepelak, "Electrochemical properties of spinel  $\text{Li}_4\text{Ti}_5\text{O}_{12}$  nanoparticles prepared via a low-temperature solid route", *J. Solid State Electr.*, 20 (2016) pp. 2673.
15. J. Shu, "Study of the Interface Between  $\text{Li}_4\text{Ti}_5\text{O}_{12}$  Electrodes and Standard Electrolyte Solutions in 0.0-5.0 V", *Electrochem. Solid-State Lett.*, 11 (2008) pp. A238.
16. T.F. Yi, L.J. Jiang, J. Shu, C.B. Yue, R.S. Zhu, H.B. Qiao, "Recent Development and Application of  $\text{Li}_4\text{Ti}_5\text{O}_{12}$  as Anode Material of Lithium Ion Battery", *J. Phys. Chem. Solids*, 71 (2010) pp. 1236.
17. S. Y. Feng, W. Feng, C. C. Feng, "Preparation of  $\text{Li}_4\text{Ti}_5\text{O}_{12}$  from Nanocrystalline  $\text{TiO}_2$  and It's Lithiation Performance", *Acta. Phys. Sin.*, 20 (2004) pp. 707.
18. Q. Y. Zhang, X. Li, "Recent Developments in the Doped-  $\text{Li}_4\text{Ti}_5\text{O}_{12}$  Anode Materials of Lithium-Ion Batteries for Improving the Rate Capability", *Int. J. Electrochem. Sci.*, 8 (2013) pp. 6449.
19. A.Y. Shenouda, K.R. Murali, "Electrochemical properties of doped Lithium titanate compounds and their performance in Lithium rechargeable batteries", *J. Power Sources*, 176 (2008) pp. 332.
20. F. Li, M. Zeng, J. Li, H. Xu, "Preparation and Electrochemical Performance of Mg-doped  $\text{Li}_4\text{Ti}_5\text{O}_{12}$  Nanoparticles as Anode Materials for Lithium-Ion Batteries", *Int. J. Electrochem. Sci.*, 10 (2015) pp. 10445.
21. J. Shuangze, J. Zhang, W. Wang, Y. Huang, Z. Feng, Z. Zhang, Z. Tang, "Preparation and effects of Mg-doping on the electrochemical properties of spinel  $\text{Li}_4\text{Ti}_5\text{O}_{12}$  as anode material for Lithium ion battery", *Mater. Chem. Phys.*, 123(2010) pp. 510.
22. W. N. Wei, H. Z. Chun, C. X. Mei, W. Zhao-yu, "Effects of  $\text{Mg}^{2+}$  Doping on Performance of Anode Material  $\text{Li}_4\text{Ti}_5\text{O}_{12}$ ", *J. Adv. Mater. Res.*, 779-780 (2013) pp.307.
23. L. Shi, X. Hu, Y. Huang, "Fast microwave-assisted synthesis of Nb-doped  $\text{Li}_4\text{Ti}_5\text{O}_{12}$  for high-rate Lithium-ion batteries", *J. Nanopart Res.*, 16 (2014) pp. 2332.
24. M. Ganesan, M. V. T. Dhananjeyan, K. B. Sarangapani, N. G. Renganathan, "Solid state rapid quenching method to synthesize micron size  $\text{Li}_4\text{Ti}_5\text{O}_{12}$ ", *J. Electroceramics*, 18 (2007) pp.329.
25. B. Vikram Babu, K.V. Babu, G.T. Aregai, L.S. Devi, B. M. Latha, M. S. Reddi, K. Samatha, V. Veeraiah, "Structural and Electrical properties of  $\text{Li}_4\text{Ti}_5\text{O}_{12}$  anode material for Lithium-ion batteries", *Results Phys.*, 9 (2018) pp.284.
26. J. Wolfenstine, and J. L. Allen, "Electrical Conductivity and Charge Compensation in Ta doped  $\text{Li}_4\text{Ti}_5\text{O}_{12}$ ", *J. Power Sources*, 180 (2008) pp. 582.
27. M. Wilkening, R. Amade, W. Iwaniak, and P. Heitjans, "Ultraslow Li diffusion in spinel type structured  $\text{Li}_4\text{Ti}_5\text{O}_{12}$ . A comparison of results from solid state NMR and impedance spectroscopy", *Phys. Chem. Chem. Phys.*, 9 (2007) pp. 1239.
28. W. N. Wei, H. Z. Chun, C. X. Mei, and W. Zhao-yu, "Effects of  $\text{Mg}^{2+}$  Doping on Performance of Anode Material  $\text{Li}_4\text{Ti}_5\text{O}_{12}$ ", *Advanced Materials Research*, 779-780 (2013) pp. 307.
29. J. M. Tarascon, M. Armand, "Issues and challenges facing rechargeable Lithium batteries", *Nature*, 414 (2001) pp. 359.
30. S. Prakash, P. Manikandan, K. Ramesha, M. Sathiya, J.M. Tarascon, and A. K. Shukla, "Solution-Combustion Synthesized Nanocrystalline  $\text{Li}_4\text{Ti}_5\text{O}_{12}$  As High-Rate Performance Li-Ion Battery Anode", *Chem. Mater.*, 22 (2010) pp. 2857.